Nat. Hazards Earth Syst. Sci. Discuss., 2, 4581–4608, 2014
www.nat-hazards-earth-syst-sci-discuss.net/2/4581/2014/
doi:10.5194/nhessd-2-4581-2014

Natural Hazards and Earth System Sciences
Discussions
Open Access

The use of FLO2D numerical code in lahar hazard evaluation at Popocatépetl volcano: a 2001-lahar scenario

L. Caballero and L. Capra

Centro de Geociencias, UNAM, Blvd. Juriquilla No. 3001. Querétaro, 76230, México, Querétaro, Mexico

Received: 6 June 2014 – Accepted: 15 June 2014 – Published: 4 July 2014

Correspondence to: L. Caballero (lcaballero@geociencias.unam.mx)

Published by Copernicus Publications on behalf of the European Geosciences Union.

Abstract

Lahar modelling represents an excellent tool to design hazard maps. It allows the definition of potential inundation zones for different lahar magnitude scenarios and sediment concentrations. Here we present the results obtained for the 2001 syneruptive lahar at Popocatépetl volcano, based on simulations performed with FLO2D software. An accurate delineation of this event is needed since it is one of the possible scenarios considered during a volcanic crisis.

One of the main issues for lahar simulation using FLO2D is the calibration of the input hydrograph and rheologic flow properties. Here we verified that geophone data can be properly calibrated by means of peak discharge calculations obtained by superelevation method.

Simulation results clearly show the influence of concentration and rheologic properties on lahar depth and distribution. Modifying rheologic properties during lahar simulation strongly affect lahar distribution. More viscous lahars have a more restricted aerial distribution, thicker depths, and resulting velocities are noticeable smaller.

FLO2D proved to be a very successful tool to delimitate lahar inundation zones as well as to generate different lahar scenarios not only related to lahar volume or magnitude but also to take into account different sediment concentrations and rheologies widely documented to influence lahar prone areas.

1 Introduction

Lahar phenomena represent one of the major threats at volcanoes. They are mixtures of water and sediments that flow on volcano slopes (Smith and Fritz, 1989) remobilizing old and new volcanic products. Their triggering mechanisms include glacial melting during volcanic activity, intense rainfall or dam-break. These triggering mechanisms allowed them to occur without being related to volcanic eruptions which makes them very hazardous. Lahars have caused several catastrophes worldwide vastly reported

NHESSD
2, 4581–4608, 2014

in literature (Voight, 1990; Siebe, 1996; Lavigne et al., 2000; Scott et al., 2005). Additionally, small eruptions can trigger very large events (i.e. 1985 Nevado del Ruiz eruption, Williams, 1987). Based on these facts, several tools need to be used in order to precisely delimitate lahar inundation zones around volcanoes and minimize our vulnerability to this phenomena.

Areas prone to lahar inundation can be adequately delineated by different methods. Field data is useful in our understanding of the magnitude and distal reach of past events in a specific volcano but it has the disadvantage that in very active gullies lahar deposits are easily eroded by subsequent events (i.e Graettinger et al., 2010). Misinterpretation of lahar deposits including their magnitude and recurrence could lead to exclude some areas that could be affected during major events. In recent years, one of the major instruments used to replicate old events and accurately delineate lahar active paths is lahar modelling (i.e. Iverson et al., 1998; Davila et al., 2007; Muñoz-Salinas et al., 2009a; Williams et al., 2008; Worni et al., 2012). Different simulations codes include LaharZ (Schilling, 1998), Titan2D two-phase flow (Williams et al., 2008), and FLO2D (O'Brien, 1993). All of them have been documented to reproduce with a high degree of accuracy lahar events.

In this work, the 2001 lahar occurred at Popocatépetl volcano just after the emplacement of a pumice flow from a 8 km eruptive column is modeled using FLO2D numerical code (O'Brien, 1993), a tool recently successfully used to simulate debris flows in volcanic environments (Worni et al., 2012). FLO2D allows reproduction of debris and hiperconcentrated flows and offers the advantage of modifying flow sediment concentration and debris flow rheology, factor that influence lahar distribution and depth. Geophone unpublished data is here used to reconstruct initial hydrograph and sediment concentration. Results obtained were compared with field data and demonstrated a good agreement in thickness and flow distribution. A comparison with previously published data related with lahar velocity (Muñoz-Salinas, 2007) is also made. Additionally, lahars with fluctuating sediment concentrations but with similar volume are simulated to observe the influence of sediment concentration and rheological behavior on lahar distribution and their hazard.

1.1 Background

Popocatépetl volcano is one of the most active volcanoes in Mexico, which activity increased since 1994, representing a threat for more than 20 million people on its surroundings. It belongs to Sierra Nevada, a N–S volcanic chain, located on the central sector of the Trans Mexican Volcanic Belt. (Fig. 1). Lahars at Popocatépetl volcano have been triggered mainly due to volcanic activity (Siebe et al., 1996; González, 2000; Capra et al., 2004; Muñoz et al., 2010). The magnitudes of these events along Popocatépetl history have varied from small lahars generated by intense rainfall (Capra et al., 2004) to very huge events that travelled more than 50 km away from the volcano associated to Plinian activity (González, 2000; Siebe et al., 1996, 1999). Large lahars triggered by major eruptions affected mexican prehispanic civilizations and their deposits are distributed where major cities, like Puebla and Cuatla, are now settled (Siebe et al., 1996).

On 7 May 2013 Popocatépetl volcano incremented the intensity of its volcanic activity with intra-crater lava dome extrusions rapidly destroyed by moderated explosions that formed columns of up to 3–4 km high. This behavior put into alert scientific community causing the raise of volcanic alert to yellow phase three by 12 May 2013 (CENAPRED, internal reports). One of the possible scenarios considered during this crisis was an event similar to the 2001 explosive activity, which was characterized by an 8 km eruptive column and the subsequent formation of pumice flows up to 6 km from the crater (Fig. 2; Sheridan et al., 2001). Partial melting of the glacier remobilized the new deposits, forming a lahar few hours after on the NE flank of the volcano, along Huiloac Gorge, almost reaching Santiago Xalitzintla town (Capra et al., 2004). A similar event occurred in 1997, when intense ash fall on top of the glacier promoted a rapid water release that resulted in a lahar that also inundated the Santiago Xalitzintla town (with more than 10 000 inhabitants) along the Huiloac-Tenenepanco ravine

(Capra et al., 2004). Nowadays a glacier is no longer present on the Popocatépetl cone (Julio-Miranda et al., 2008) but, as at other mexican active volcanoes such as the Volcán de Colima, lahars are very frequent during rainy season (Davila et al., 2007; Capra et al., 2010), especially when pyroclastic material from an ongoing activity accumulates on the upper slope of the volcano. The 2001 explosive episode probably represents the biggest eruption since 1994 when the volcano reactivated after more than 70 years of inactivity (since 1927) (Martin-Del Pozzo, 2012). The occurrence of a similar scenario make the reproduction of this event of fundamental importance, in order to accurately delimitate lahar hazard zones.

1.2 2001-lahar event

On 22 January 2001 an explosive episode (Fig. 2), characterized by an 8 km eruptive column gave place to pumice flows that emplaced mostly on the northern sector of the cone up to 4–6 km of distances from the crater (Espinasa Pereña, 2012). This episode of activity had an estimated VEI of 3–4 (Espinasa Pereña, 2012) and has been one of the most violent phases since 1994.

As the flows descended over the glacier they eroded and melted part of it, and after approximately five hours a lahar descended along the Huiloac Gorge for 15 km, almost reaching Santiago Xalitzintla town (Capra et al., 2004; Tanarro et al., 2010). Based on geophone data the event started at 22:32 and ended at 23:20 GMT. The load of the produced lahar was calculated at 1.6×10^5 m^3 and reached speeds from 1.3 to 13.8 m s^{-1} (Muñoz et al., 2007, 2009).

The deposit has been described as a massive debris flow, with an average thickness of 70 cm up to a maximum of 150 cm in the middle reach. It consists of a matrix-supported unit, with rounded to sub-rounded clasts embedded in a matrix that consist of up to 70 % of sand + silt, and up to 1 % of clay (Fig. 3). Components consist of juvenile pumices and secondary andesitic fragments (Capra et al., 2004).

Six lahars have occurred after 2001 lahar events, four of them occurred during dry season, caused by snowmelt. The others were generated in mid to final period of the

NHESSD
2, 4581–4608, 2014

rainfall season and were associated with torrential rains (Muñoz-Salinas, 2010). Based on this, lahar hazard evaluation should take into account different triggering scenarios and the sediment available for remobilization inside volcano gorges. Special attention should be paid along Huilac gorge the most active basin in regards to lahars.

2 Methodology

The FLO2D numerical model (O'Brien, 1993) routes flood hydrographs over unconfined channels solving the full dynamic wave equation. It uses an established grid over the topographic area (computational domain) and calculates flow depth and velocity between the grid elements. Flow velocity in 8 directions is calculated independently, with an algorithm that includes flow geometry, roughness (Manning n value), the slope between two grid elements, and wetted perimeter. Once the velocity is solved, it is multiplied by the cross-sectional area and discharge is calculated. Floodwave advance and direction is determined by topography and resistance to flow. Debris and hyperconcentrated flows can be simulated by a quadratic rheological model that involves sediment concentration, yield stress and viscosity terms. FLO2D predicts viscous fluid motion as a function of sediment concentration.

Input data required for mud/debris flow simulations comprises: inflow (hydrograph) and outflow cells, Manning n values, rheologic parameters (α and β), laminar flow resistance (K), and limiting Froude number. Rheologic parameters (α and β) are empirical parameters that relate yield stress and viscosity with sediment concentration by the empirical relationships (O'Brien and Julien, 1988):

$$\eta = \alpha_1 e^{\beta 1 C v}$$

$$\tau_y = \alpha_2 e^{\beta 2 C v}$$

In a FLO2D mud/debris flow simulation the water and sediment volumes as well as sediment concentrations for every grid element and time-step are computed.

NHESSD
2, 4581–4608, 2014

Analysis of the different input parameters was performed by Boniello et al. (2010), Hsu et al. (2010), and Worni et al. (2012). They include data from FLO2D user's manual, as well as back analysis to fit field and debris flow data from literature in order to obtain confident rheologic coefficients. All of their results point to DEM resolution, rheologic parameters and Manning coefficients like the most sensitive parameters for a successful simulation in FLO2D.

In this work debris flow simulation was performed using a 30 m digital elevation model. The 30 m DEM was created resampling a 5 m LiDAR DEM to use an accurate topography without substantially increasing simulation time. The grid imposed over topography for input data and FLO2D velocity calculations was also at 30 m. A 30 m DEM and grid allowed obtaining flow simulation results on the same scale.

2.1 Inflow data

For hydrograph reconstruction, data recorded from geophone stations installed by CENAPRED and USGS was used (Fig. 4). Data from geophone PFM3 was chosen because its proximity to the point where all tributary rivers converge to Huiloac gorge. Besides, Huiloac gorge has no tributary gullies hence its budget is determined by water availability behind this point (Tanarro et al., 2010).

Data from the full frequency band (10–250 Hz) was correlated with peak discharge calculations from Muñoz et al. (2007) obtained by superelevation method. To avoid surging during flow simulations, extreme peaks observed in raw data were suppressed but the overall shape of the hydrograph was maintained. The conversion from AFM units ($cm\,s^{-1} \times 10^{-6}$) to discharge units ($m^3\,s^{-1}$) was made assuming that the maximum peak discharge (Muñoz et al., 2007) corresponded to the maximum value of the hydrograph (Suwa et al., 2000). Flow concentration was established assuming a maximum flow concentration of 0.5 during the peak flow and the main body of the flow, which is in agreement with field observation and textural characteristics of the deposit (Capra et al., 2004). The recessional part of the flow was assumed to be a hyperconcentrated flow (Fig. 4).

NHESSD
2, 4581–4608, 2014

2.2 Manning *n* values

Manning values were established using USGS empirical tables. Base values of Manning's *n* for natural channels composed by cobbles and boulders range from 0.030 to 0.070 (Phillips and Tadayon, 2006) so an intermediate value of 0.05 was chosen. Huiloac gorge has different properties related to channel irregularities, channel alignment, obstructions, and vegetation so some adjustments to base *n* value were needed in order to better characterize channel roughness. Three different Manning *n* values were used, based on channel characteristics mentioned above (Fig. 5). A value of 0.064 was used for the segment were the channel is very narrow, the base is composed of cobble and boulders, and a moderate degree of irregularities is observed. Variations in channel cross sections alternates occasionally and the effects of obstructions and vegetation is negligible. Floodplain at both sides of the Huiloac gorge has severe vegetation obstructions giving a Manning value of 0.118, which is also in accordance of Chow values for floodplain analysis (1959). Last adjustment in *n* value was done where Huiloac gorge opens to different branches where channel segments are more sinuous, shallower and wider, with medium vegetation degree, giving a value of 0.081.

2.3 Rheologic coefficients α and β

Rheologic coefficients α and β were chosen based on O'Brien and Julien data (1988). Four different values of α and β for 2001-lahar were simulated in order to observe the influence of rheologic characteristics in lahar distribution (Table 1). The first scenario was based on the reproduction of the 2001-lahar. Values α and β were chosen using the sample with more similar granulometric composition of this lahar corresponding to Glenwood 2 sample, also in accordance to values used in previous works (Worni et al., 2012). The second scenario was a more diluted lahar, α and β values were maintained and only a hydrograph with minor sediment concentration was used. Third and fourth scenarios were done for more viscous lahars, and α and β values correspond to samples with more clay content in order to raise yield strength and viscosity of the flow. A clay content of 4.8 (Glenwood 3 sample) and 6.8 (Glenwood 1 sample) was used for simulations 3 and 4 respectively.

2.4 Laminar flow resistance (K) and limiting Froude number (F)

During all simulations a limiting Froude number of 0.9 was set to maintain a subcritic flow regime. Laminar flow resistance value was set in 2000 according to the values suggested in the user's guide based on substrate characteristics.

3 Results

3.1 2001 event

Results of 2001-lahar simulation obtained by FLO2D are shown in Fig. 6. Four aspects were compared between simulation and field and indirect estimated data (Muñoz-Salinas, 2007) to observe simulation accuracy: spatial distribution, flow depth, flow velocity, and flow volume.

Flow simulation reaches approximately 10 km from the hydrograph point, and stops almost 800 m before reaching Santiago Xalitzintla town. Although lasts outcrops of 2001-lahar deposit are found approximately 3.5 km before Santiago Xalitzintla town (Fig. 1), distal reaches obtained by FLO2D simulation would represent the watery recessional parts of the lahar since flow depths at these points is less than 50 cm. Flow depth comparison was made using river transversal profiles and stratigraphic columns described by Capra et al. (2004). River profiles (Fig. 6) show flow depths obtained during simulations and deposit thickness at the same point. Flow depths in proximal reach range from 1.0 to 1.9 m while deposit thickness is reported from 0.5 to 0.8 m. At medial reach, simulation gives a maximum flow depth of 1.5 and deposit thickness is about 0.7 m. Distal part of the simulation has a maximum flow depth of 1 m and deposit thickness varies widely from 0.5 to 0.12 m. Flow depths consider sediment plus water

NHESSD
2, 4581–4608, 2014

so inundation line must be always above the deposit. Considering a 0.5 concentration of sediment of the flow, FLO2D reproduces well enough lahar flow depths along the entire deposit (Fig. 6). Some problems were encountered with the portion of the flow where the maximum curvature of the gullie is observed. Field data at this point shows maximum deposit thickness of 1.9 m while flow depths achieved during simulation vary between 1–1.5. The geometry of the deposit suggests that at this zone the flow geometry was modified by local conditions. In this part of the gully, the 2001-lahar was deposited on top of older terraces so FLO2D was not able to reproduce this behavior. Hence, DEM resolution could also emphasize this effect.

Lahar velocity distribution observed during flow simulations were compared with velocity data reported by Muñoz et al. (2007) by superlevation method (Fig. 7). Maximum lahar velocities calculated by FLO2D are circa of 6.2 $m\,s^{-1}$ and are achieved in proximal facies. Muñoz et al. (2007) estimated velocities between 13.8 and 1.5 $m\,s^{-1}$ for 2001-lahar. A mean value of 5.65 $m\,s^{-1}$ is obtained from these data in points located along lahar simulation. Considering the wide range of estimated velocities and the error estimated for superlevation method of 15 % (Pierson, 1985) velocities estimated during lahar simulation are a good approximation of estimated flow velocities.

Finally, flow volume calculated by FLO2D is of circa 4.1×10^5 m^3 (water bulked with sediments). The mean amount of water is 2.5×10^5 m^3 and sediment volume is 1.6×10^5 m^3, considering the longitudinal profile in sediment concentration from the hydrograph input data (Fig. 3). Capra et al. (2004) and Muñoz-Salinas et al. (2009b) estimated lahar volume within $1.6–2.3 \times 10^5$ m^3 that is of the same order of magnitude of that calculated by FLO2D.

Based on previous statements results of FLO2D 2001-lahar simulation are in good agreement with previous works.

3.2 Different lahar scenarios at Popocatéptl volcano

Flow simulations allow the generation of different lahar scenarios. These scenarios should be created based on the magnitude of past events and the present conditions on lahar active paths. Most of lahar simulations are magnitude-based scenarios or reproduction of some events (Aguilera et al., 2004; Williams et al., 2008; Worni et al., 2012). Strong variations on lahar sediment concentration or transformation from debris flow to hyperconcentrated flow or vice versa can occur (Pierson and Scott, 1985). Based on this, we believe that different scenarios should consider different sediment concentrations for lahars of the same magnitude, since this characteristic will influence travel distance and therefore will strongly influence hazard maps.

Since its reactivation in 1994, largest lahars generated at Popocatépetl volcano along Huiloac gorge, were triggered by peaks in volcanic activity that melted part of the glacier. Most hazardous scenarios are similar to the 1997 and 2001 lahars with flow volumes estimated between 2 and 3.3×10^5 m^3 (Capra et al., 2004; Muñoz-Salinas et al., 2009b). In addition, based on lahars occurred at Popocatepetl volcano in 1997 and 2001; Capra et al. (2004) point to the evidence that depending on the nature of the material contributing to the initiation of a lahar, the flow behavior can highly change, mostly depending on fine (silt and clay) content. The 1997 lahar was fine depleted and rapidly diluted to a hyperconcentrated flow at the same distance where the 2001 was still maintaining a high sediment concentration in the range of a debris flow. Therefore, fine sediment content influences dynamic behavior, transformations and dynamic rheologic behavior.

FLO2D allows modifying concentration and rheologic properties of the lahars modifying initial input hydrograph and α and β coefficients. Based on that, α and β coefficients and sediment concentration were adapted to consider these possible different behaviors observed in 1997 and 2001 lahars (Table 1). Three alternative scenarios (AS) were proposed for events of the same magnitude as 2011-lahar. AS1 with lower sediment concentration but the same rheologic coefficients of 2001-lahar. AS2 with rheologic properties equivalent to a fine content of 4.8 %. Finally, AS3 with rheologic properties equivalent to a fine content of 6.8 %. Sediment concentration of AS2 and AS3 was the same of 2001-lahar.

NHESSD
2, 4581–4608, 2014

Simulation results, which include inundation areas, flow depths and velocities, are presented in Figs. 8 and 9. It is clear to see the influence of sediments concentration and rheologic properties on lahar distribution, depth and velocity. It is worth to mention that no variation in flow width is seen related to rheological properties of the lahar. AS1, the more diluted lahar (Figs. 8a and 9a), gives a spatial distribution and flow depths very similar to that of 2001. Lahar concentration affected mainly flow velocity that reaches a maximum of 4.6 $m\,s^{-1}$ compared to 6.2 $m\,s^{-1}$ of 2001-scenario. AS2, a more viscous lahar, has a more restricted aerial distribution, and it stops approximately 3 km before reaching Santiago Xalitzintla town (Figs. 8a and 9b). In the proximal parts it achieves almost 2.7 m of flow depth with a clear steepest front. There is no recessional watery part of the flow like in more diluted 2001-lahar. Resulting velocities are noticeable smaller reaching a maximum value of 4.6 $m\,s^{-1}$. AS3, the more viscous lahar scenario (Table 1, Fig. 8a and 9c) reaches a maximum flow depth of 3.5 m almost twice thicker than that of 2001-lahar. It stops at 3.5 km before arriving Santiago Xalitzintla town and is the slowest lahar with a maximum velocity of 3.6 $m\,s^{-1}$.

A comparison of 2001-lahar simulation and the alternative scenarios shows how important is to consider sediment concentration and rheologic properties of lahars for hazard evaluation (Fig. 8). Differences in distal reaches are up to 3.5 km between more diluted and more viscous lahars. Inundation area of the more diluted lahar (AI1) is almost twice, compared with the more viscous scenario (AI3). Standard deviation of flow depths, obtained with a point analysis, clearly shows that rheologic properties can cause strong differences in flow depth, especially in proximal facies of the lahar (Fig. 8b).

Based on the above, it is important to consider these strong differences when lahar hazard maps are made. A final map integrating the results of 2001-lahar and the alternative scenarios simulated is shown in Fig. 10. The map uses the maximum flow depths at each cell based on the four different scenarios here simulated and the maximum aerial distribution.

4 Discussion and conclusions

Lahar modelling represents an excellent tool to design hazard maps. It allows, if they are properly calibrated, the definition of potential inundation zones for different lahar magnitude scenarios and sediment concentrations.

Results presented here proved FLO2D as a useful tool in lahar modelling at Popocatépetl volcano. A very good agreement between field data (Capra et al., 2004), flow behavior (Muñoz et al., 2009), and 2001-lahar simulation were observed. One of the main issues for lahar simulation using FLO2D is the calibration of the input hydrograph. Here we verified that geophone data could be properly calibrated by means of peak discharge calculations obtained by superelevation method.

Lahars in active volcanoes represent a major threat. They can be triggered by volcanic activity i.e. glacier melting, by intense rainfall, by a crater dam-break or by the transformation of debris avalanches into these phenomena. The consequences of such diverse scenarios are lahars with important variations in sediment concentration and behaviors, varying between debris and hyperconcetrated flows. Both types of flows have different dynamic and rheological behaviors resulting in different flow velocities and maximum runout, for hence, they represent different threats. One of the shortcomings of lahar modeling is the creation of different scenarios based only on lahar magnitude. Results of lahar simulation presented here for 2001-lahar involve lahars of the same magnitude but with different sediment concentration and fine content. Difference in travel distances is up to 3.5 km for events of the same magnitude and maximum flow depths can have differences of more than 1 m. Besides, modifications in lahar rheology not only affect its distribution, they also modify flow thickness and velocities. More viscous lahars have more restricted distribution but are deeper than more fluid ones as it is observed by different scenario simulations.

Results of lahar modelling can be made with an uncertainty of 2–4 km (Huggel et al., 2008). This effect could be enhanced by not taking into account lahar rheology.

NHESSD
2, 4581–4608, 2014

Modeling lahar events based only on volumes can enhance the uncertainty in the results, but this can be avoided by recreating different rheologic scenarios.

FLO2D proved to be a very successful tool to delineate lahar inundation zones as well as to generate different lahar scenarios not only related to lahar volume or magnitude but also to take into account different sediment concentrations and rheologies widely documented to influence lahar prone areas.

Acknowledgements. This work was partially founded by Conacyt 99486 project (to Lucia Capra), and by a postdocotoral fellowship from DGAPA-UNAM to Lizeth Caballero. Seismic data of the 2001-lahar were provided by Ing. Gilberto Castellan, Centro Nacional de Prevención de Desastres.

References

Aguilera, E., Pareschi, M. T., Rosi, M., and Zanchetta, G.: Risk from lahars in the Northern Valleys of Cotopaxi Volcano (Ecuador), Nat. Hazards, 33, 161–189, 2004.

Boniello, M. A., Calligaris, C., Lapasin, R., and Zini, L.: Rheological investigation and simulation of a debris-flow event in the Fella watershed, Nat. Hazards Earth Syst. Sci., 10, 989–997, doi:10.5194/nhess-10-989-2010, 2010.

Capra, L., Poblete, M. A., and Alvarado, R.: The 1997 and 2001 lahars of Popocatépetl volcano (Central Mexico): textural and sedimentological constraints on their origin and hazards, J. Volcanol. Geoth. Res., 131, 351–369, 2004.

Capra, L., Borselli, L., Varley, N., Gavilanes-Ruiz, J. C., Norini, G., Sarocchi, D., Caballero, L., and Cortes, A.: Rainfall-triggered lahars at Volcán de Colima, Mexico: surface hydro-repellency as initiation process, J. Volcanol. Geoth. Res., 189, 105–107, 2010.

Chow, V. T.: Open-channel hydraulics, in: Open-Channel Hydraulics, McGraw-Hill, 109–113, USA, 1959.

Davila, N., Capra, L., Gavilanes-Ruiz, J. C., Varley, N., Norini, G., and Gómez Vazquez, A.: Recent lahars at Volcán de Colima (Mexico): drainage variation and spectral classification, J. Volcanol. Geoth. Res., 165, 127–141, 2007.

Espinasa Pereña, R.: Historia de la actividad del Volcán Popocatépetl 17 años de erupciones, CENAPRED, 69, Mexico, 2012.

Gonzalez, A.: Estudios de detalle estratigráfico y sedimentológico del Lahar de San Nicolás en el flanco noreste del volcán Popocatépetl, Undergraduate, Facultad de Ingeniería, UNAM, 110 pp., Mexico City, Mexico, 2000.

Graettinger, A. H., Manville, V., and Briggs, R. M.: Depositional record of historic lahars in the upper Whangaehu Valley, Mt. Ruapehu, New Zealand: implications for trigger mechanisms, flow dynamics and lahar hazards, B. Volcanol., 72, 279–296, 2010.

Hsu, S. M., Chiou, L. B., Lin, G. F., Chao, C. H., Wen, H. Y., and Ku, C. Y.: Applications of simulation technique on debris-flow hazard zone delineation: a case study in Hualien County, Taiwan, Nat. Hazards Earth Syst. Sci., 10, 535–545, doi:10.5194/nhess-10-535-2010, 2010.

Huggel, C., Schneider, D., Miranda, P. J., Delgado Granados, H., and Kääb, A.: Evaluation of ASTER and SRTM DEM data for lahar modeling: a case study on lahars from Popocatépetl Volcano, Mexico, J. Volcanol. Geoth. Res., 170, 99–110, 2008.

Iverson, R. M., Schilling, S. P., and Vallance, J. W.: Objective delineation of lahar hazard zones, Geol. Soc. Am. Bull., 110, 972–984, 1998.

Julio-Miranda, P., Delgado, H., Huggel, C., and Kraab, A.: Impact of the eruptive activity on galcier evolution at Popoactépetl Volcano (México) during 1994–2004, J. Volcanol. Geoth. Res., 170, 86–98, 2008.

Lavigne, F., Thouret, J., Voight, B., Suwa, H., and Sumaryono, A.: Lahars at Merapi volcano, Central Java: an overview, J. Volcanol. Geoth. Res., 100, 423–456, 2000.

Martin-Del Pozzo, A. L.: Precursors to eruptions of Popocatépetl Volcano, Mexico, Geofis. Int., 51, 87–107, 2012.

Muñoz-Salinas, E., Manea, V. C., Palacios, D., and Castillo-Rodriguez, M.: Estimation of lahar flow velocity on Popocatépetl volcano (Mexico), Geomorphology, 92, 91–99, doi:10.1016/j.geomorph.2007.02.011, 2007.

Muñoz-Salinas, E., Castillo-Rodríguez, M., Manea, V., Manea, M., and Palacios, D.: Lahar flow simulations using LAHARZ program: application for the Popocatépetl volcano, Mexico, J. Volcanol. Geoth. Res., 182, 13–22, 2009a.

Muñoz-Salinas, E., Renschler, C., and Palacios, D.: A GIS-based method to determine the volume of lahars: Popocatépetl volcano, Mexico, Geomorphology, 111, 61–69, 2009b.

Muñoz-Salinas, E., Castillo-Rodriguez, M., Manea, V., Marina, M., and Palacios, D.: On the geochronological method versus flow simulation software application for lahar risk mapping: a case study of Popocatepetl volcano, Mexico., Geogr. Ann. A, 92, 311–328, 2010.

NHESSD
2, 4581–4608, 2014

A 2001-lahar scenario

L. Caballero and L. Capra

O'Brien, J. and Julien, P.: Laboratory analysis of mudflow properties, J. Hydraul. Eng.-ASCE, 114, 877–887, 1988.
O'Brien, J., Julien, P., and Fullerton, W.: Two-dimensional water flood and mudflow simulation, J. Hydraul. Eng.-ASCE, 119, 244–261, 1993.
Phillips, J. V. and Tadayon, S.: Selection of Manning's roughness coefficient for natural and constructed vegetated and non-vegetated channels, and vegetation maintenance plan guidelines for vegetated channels in Central Arizona, US Department of the Interior, USGS, Reston, Virginia, USA, 2006.
Pierson, T. C.: Initiation and flow behavior of the 1980 Pine Creek and Muddy River lahars, Mount St. Helens, Washington, Geol. Soc. Am. Bull., 96, 1056–1069, 1985.
Pierson, T. C. and Scott, K. M.: Downstream dilution of a lahar: transition from debris flow to hyperconcentrated streamflow, Water Resour. Res., 21, 1511–1524, 1985.
Schilling, S.: LAHARZ: GIS programs for automated mapping of lahar-inundation hazard zones, OFR 98–638, USGS, Vancouver, WA, 1998.
Scott, K. M., Vallance, J. W., Kerle, N., Macías, J. L., Strauch, W., and Devoli, G.: Catastrophic, precipitation-triggered lahar at Casita volcano, Nicaragua: ocurrence, bulking and transformation, Earth Surf. Proc. Land., 30, 59–79, 2005.
Sheridan, M. F., Bursik, M. I., Abrams, M., Macías, J. L., and Delgado, H.: Gauging short-term volcanic hazards at Popocatépetl, EOS Trans., 82, 185–189, 2001.
Siebe, C., Abrams, M., Macías, J. L., and Obenholzner, J.: Repeated volcanic disasters in Prehispanic time at Popocatépetl, central Mexico: past key to the future, Geology, 24, 399–402, 1996.
Siebe, C., Schaaf, P., and Urrutia-Fucugauchi, J.: Mammoth bones embedded in a late Pleistocene lahar from Popocatépetl volcano, near Tocuila, central Mexico, Geol. Soc. Am. Bull., 111, 1550–1562, 1999.
Smith, G. A. and Fritz, W. J.: Volcanic influences on terrestrial sedimentation, Geology, 17, 375–376, 1989.
Suwa, H., Yamakoshi, T., and Sato, K.: Relationship between debris-flow discharge and ground vibration, in: Proceedings of the Second International Conference on Debris-flow Hazards Mitigation: Mechanics, Prediction, and Assessment, Taipei, Taiwan, 16–18, August, 2000.
Tanarro, L. M., Andrés, N., Zamorano, J. J., Palacios, D., and Renschler, C. S.: Geomorphological evolution of a fluvial channel after primary lahar deposition: Huiloac Gorge, Popocatépetl volcano (Mexico), Geomorphology, 122, 178–190, 2010.

Voight, B.: The 1985 Nevado del Ruiz volcano catastrophe: anatomy and retrospection, J. Volcanol. Geoth. Res., 42, 151–188, 1990.
Williams, R., Stinton, A. J., and Sheridan, M. F.: Evaluation of the Titan2D two-phase flow model using an actual event: case study of the 2005 Vazcún Valley Lahar, J. Volcanol. Geoth. Res., 177, 760–766, 2008.
Williams, S. N.: Nevado del Ruiz volcano, Colombia: the November 1985 eruption and related events, J. Volcanol. Geoth. Res., 33, 355–360, 1987.
Worni, R., Huggel, C., Stoffel, M., and Pulgarín, B.: Challenges of modeling current very large lahars at Nevado del Huila Volcano, Colombia, B. Volcanol., 74, 309–324, 2012.

NHESSD
2, 4581–4608, 2014

A 2001-lahar scenario

L. Caballero and L. Capra

Table 1. Values of rheologic coefficients used for the different flow scenarios. Yield strength and viscosity were obtained by the empirical formulas used by FLO2D and from O'Brien and Julien (1988) a Empirical formulas are in the methodology section.

Simulation	Yield Strength Alfa	Yield Strength Beta	Viscosity Alfa	Viscosity Beta	Yield Strength (dynes cm^{-2})[a]	Viscosity (poises)[a]
2001-lahar	0.0765	16.9	0.0648	6.2	57.32165463	0.7348234
AS1	0.0765	16.9	0.0648	6.2	14.14629726	0.4397933
AS2	0.00071	29.8	0.00632	19.9	82.82718232	15.330482
AS3	0.0345	20.1	0.00283	23	90.45813296	23.102018

NHESSD
2, 4581–4608, 2014
A 2001-lahar scenario
L. Caballero and L. Capra

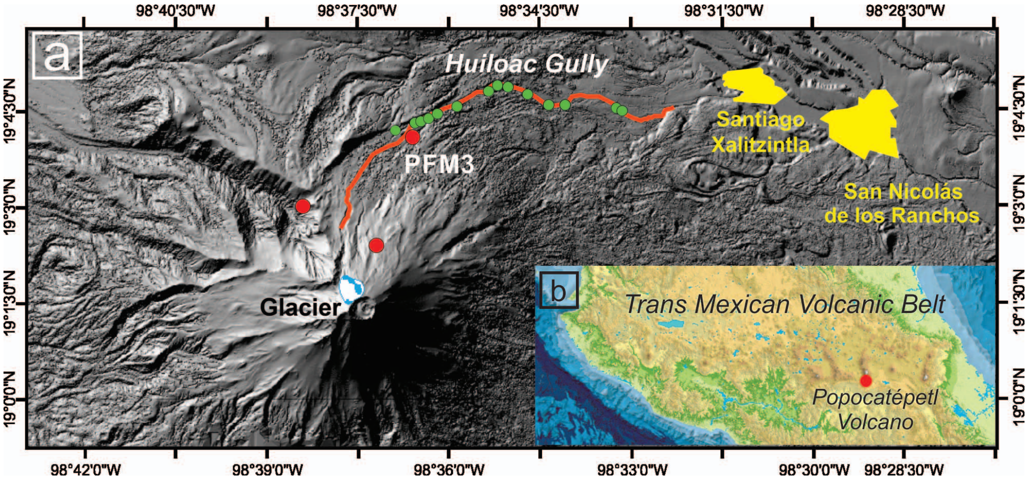

Figure 1. (a) Localization of Popocatépetl volcano in the Trans Mexican Volcanic Belt. **(b)** Popocatépetl volcano. Orange line represents 2001 lahar deposit distribution. Red circles are CENAPRED geophone locations. Green circles indicate location of stratigraphic sections collected by Capra et al. (2004).

NHESSD
2, 4581–4608, 2014

Title Page
Abstract | Introduction
Conclusions | References
Tables | Figures
◀| |▶
◀ ▶
Back | Close
Full Screen / Esc
Printer-friendly Version
Interactive Discussion

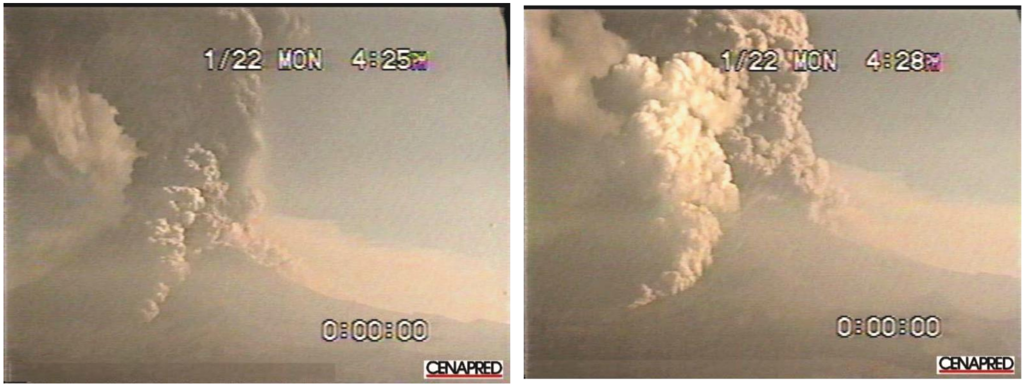

Figure 2. Photographs of 2001 eruptive activity. Pyroclastic flows flowed downslope causing glaciar melting and triggering the 2001 lahar (Photograph taken from Espinasa Pereña, 2012).

NHESSD
2, 4581–4608, 2014

L. Caballero and L. Capra

NHESSD
2, 4581–4608, 2014

Figure 3. Photographs of 2001 lahar deposit. **(a)** Proximal facies of the deposit. **(b)** Texture of 2001-lahar deposit where the massive structure and clasts dispersed in a sand-silty matrix are observable.

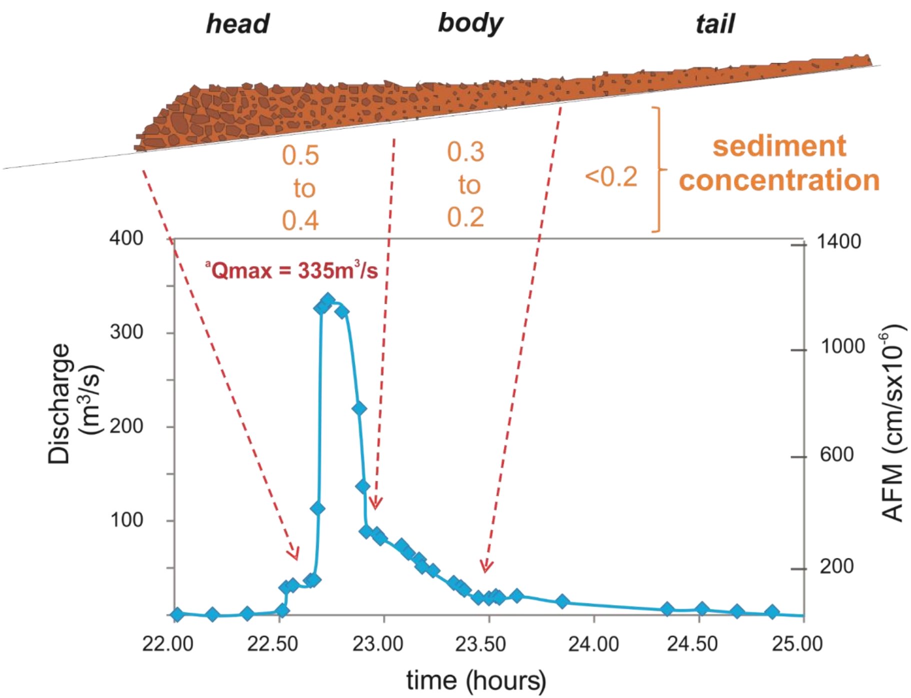

Figure 4. Geophone data used to reconstruct hydrograph of the 2001-lahar. Qmax used to calibrate geophone data was obtained by Muñoz et al. (2007). Left scale is referring to the flow discharge ($m^3 s^{-1}$). Right scale AFM units. In the upper part sediment concentration for each portion of the hydrograph is indicated. Geophone data is from CENAPRED.

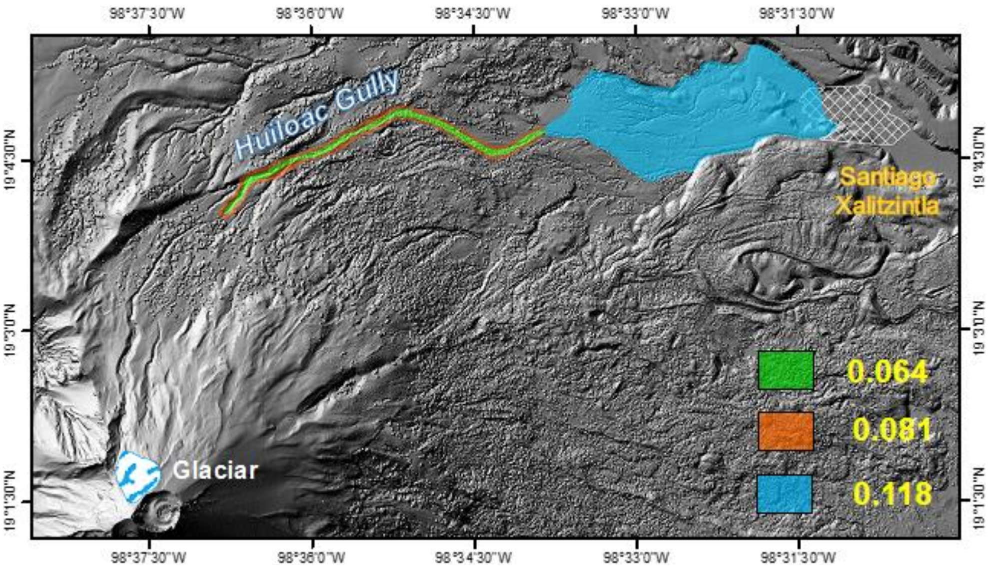

Figure 5. Distribution of manning coefficients used during FLO2D simulations.

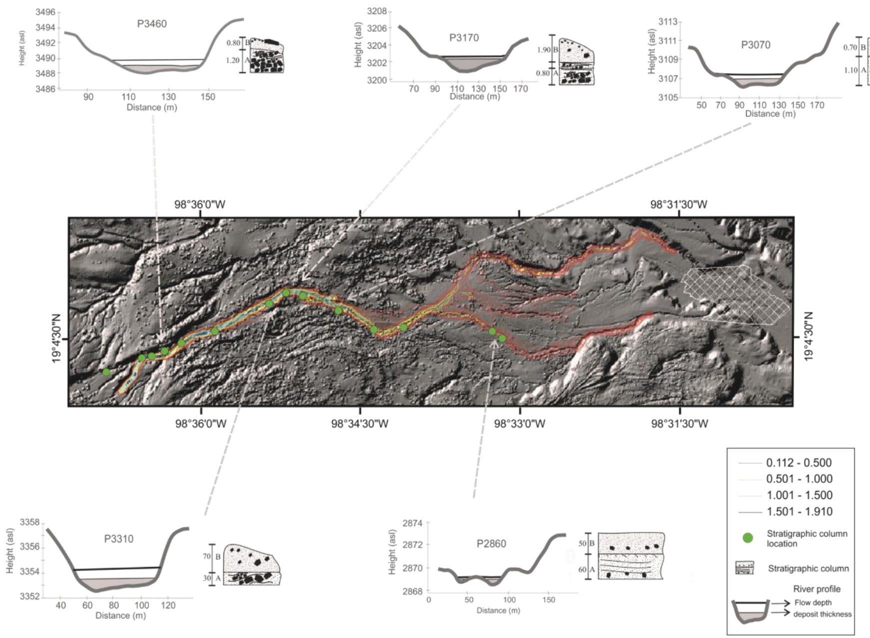

Figure 6. Simulation results of 2001-lahar for flow depth. Green circles correspond with field data published by Capra et al. (2004). Red circle is geophone PFM3 from CENAPRED. Flow sections compare flow depths calculated by FLO2D with field data collected by Capra et al. (2004). Shaded areas represent 2001-lahar deposit. Unit A refers to 1997-lahar deposit and Unit B to the 2001-lahar deposit.

NHESSD
2, 4581–4608, 2014

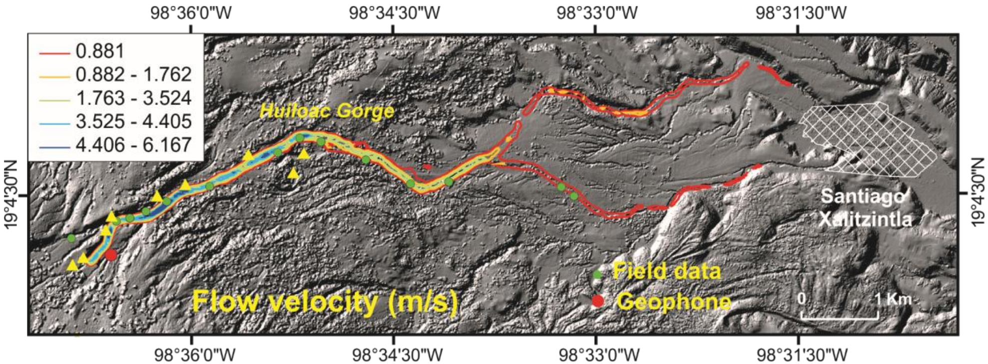

Figure 7. Velocity distribution obtained during flow simulation. Yellow triangles refer to the locations of flow velocity calculated by Muñoz et al. (2007) used here for comparison.

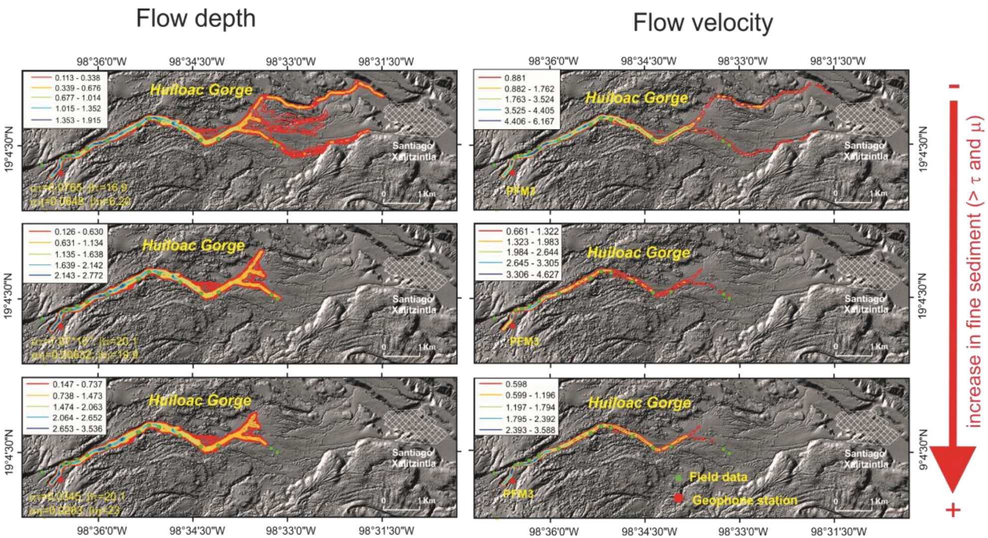

Figure 8. Results of alternative scenarios for lahars with equivalent volume of 2001-lahar but with different sediment concentrations or rheologic properties. **(a)** AS1, more diluted lahar. **(b)** AS2, lahar with 4.8 wt% of clay. **(c)** AS3, lahar with 6.8 wt% of clay. AS2 and AS3 represent high yield strength, more viscous lahars. First column represents flow depth, second column, flow velocity. Green circles correspond with field data published by Capra et al. (2004). Red circle is geophone PFM3 from CENAPRED.

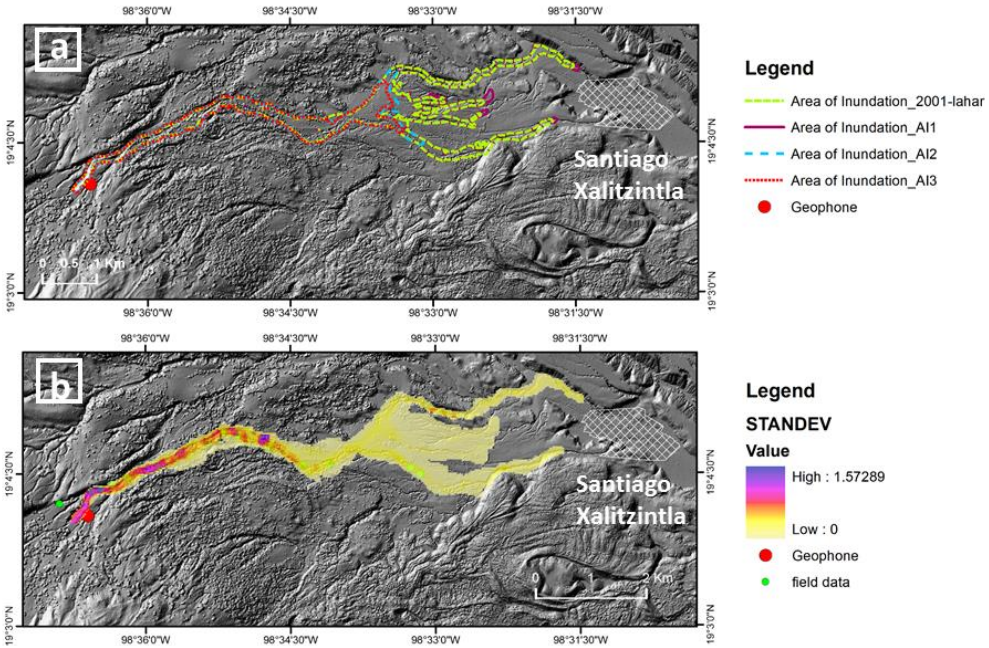

Figure 9. Comparison of the alternative scenarios with 2001-lahar simulation. **(a)** Area of inundation. **(b)** Standard deviation of flow depths.

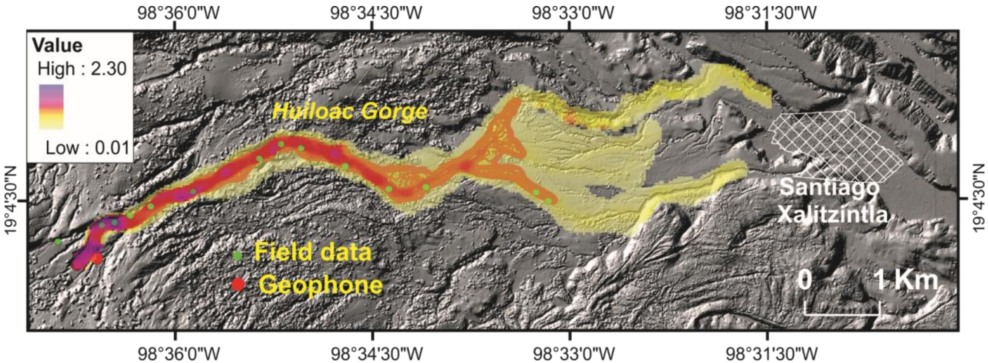

Figure 10. Final map constructed based on maximum flow depths from the different lahar scenarios here simulated.

NHESSD
2, 4581–4608, 2014

A 2001-lahar scenario

L. Caballero and L. Capra